Theor Chem Acc (1998) 100:51–59
DOI 10.1007/s002149800m44

Theoretical
Chemistry Accounts

Regular article

Spin-orbit and spin-spin couplings in He_2 and He_2^-*

N. Bjerre[1], A.O. Mitrushenkov[2], P. Palmieri[3], P. Rosmus[4]

[1] Institute of Physics and Astronomy, University of Aarhus, DK-8000 Aarhus C, Denmark
[2] Department of Theoretical Physics, Institute of Physics, St. Petersburg University, 198904 St. Petersburg, Russia
[3] Dipartimento di Chimica Fisica ed Inorganica, Università di Bologna, Viale Risorgimento 4, I-40136 Bologna, Italy
[4] Theoretical Chemistry Group, Univerisitè Marne la Vallè, F-93166 Noisy-le-Grand, France

Received: 14 April 1998 / Accepted: 27 July 1998 / Published online: 19 October 1998

Abstract. The spin-orbit and the spin-spin coupling constants of the $^4\Pi_g$ state of the He_2^- ion, of the parent $a^3\Sigma_u^+$, and of the $b^3\Pi_g$ states of He_2 have been evaluated by a multireference configuration interaction method. The theoretical spin-spin splittings of the $a^3\Sigma_u^+$ state and the *R*-dependent spin-spin function are found to be in excellent agreement with experiment, with deviations in the range of a few MHz. The theoretical spin-orbit constants and splittings of the $b^3\Pi_g$ state are larger than the experimental values by about 370 MHz. The spin-orbit coupling constant of the $^4\Pi_g$ state of He_2^- is estimated to be three times smaller than in the $b^3\Pi_g$ state, but one of the intramultiplet off-diagonal spin-spin interactions is predicted to give a large contribution to the fine structure of the metastable ion. The theoretical fine structure constants for the He_2^- ion are expected to aid future spectroscopic investigations of the fine structure splittings of the negative ion.

Key words: Autoionization – Fine structure – Spin-spin interactions

1 Introduction

There is a class of metastable negative ions with decay lifetimes of several hundreds of microseconds, in which the electronic state of the ion lies below its parent excited state and autoionizes by weak interactions with the continuum of high angular momentum. The long lifetimes permit an easy detection of the ions and allow experimental studies of the fine structure of these species. For instance, the He^- ion in the $1s2s2p\ ^4P$ state was first detected in 1939 by mass spectrometry [1] and its fine structure splittings were investigated by radiofrequency (RF) resonance spectroscopy in 1972 [2]. The $J = \frac{1}{2}$ and $J = \frac{3}{2}$ levels decay to the $1s^2\ ^1S$ ground state of He by emitting an $\epsilon\ p$ wave, whereas the $J = \frac{5}{2}$ level decays only by emitting an $\epsilon\ f$ wave, yielding a much lower decay rate. In fact, the lifetimes have been recently determined in a storage ring to be $350 \pm 15\,\mu s$ for $J = \frac{5}{2}$ [3] and $13 \pm 3\,\mu s$ for $J = \frac{3}{2}, \frac{1}{2}$ [4], in very good agreement with the most recent and very detailed theoretical treatment of the decaying levels [5, 6]. Similarly, the long-lived metastable He_2^- ion was first observed in 1984 [7]. The $^4\Pi_g$ state has the electronic configuration $1\sigma_g^2 1\sigma_u 2\sigma_g 1\pi_u$; the long-lived autodetaching component has a lifetime of $135 \pm 15\,\mu s$ and the short-lived components have lifetimes in the range of 15–30 μs. It has been suggested that the longest lifetime can be attributed to the $^4\Pi_g^-$ Λ doubling component decaying via the $^2\Delta_g$ continuum [8, 9].

The knowledge of the spin-orbit and spin-spin spectroscopic constants is of considerable interest for the detection and interpretation of the fine structure of the He_2^- ion. Even though these constants are expected to be very small, ab initio techniques using the internally contracted [10, 11] and uncontracted [12] multireference configuration interaction (MRCI) methods can provide accurate values of the molecular parameters. In order to estimate the accuracy which can be reached in the calculations, we have investigated the fine structure of the lowest Rydberg states of the neutral He_2 molecule, $a^3\Sigma_u^+$ and $b^3\Pi_g$, and of the atomic states which correlate asymptotically with the two molecular electronic states, for which experimental data are available.

The Rydberg states of the He_2 molecule were first discovered in 1913 [13, 14]. In fact, the $a^3\Sigma_u \rightarrow b^3\Pi_g$ transition around 4768 cm^{-1}, with a transition moment of about 6.9 Debye [23], is one of the most intense transitions known in the infrared (IR) spectral region. Numerous experimental [15–19] and theoretical [21–25] studies of the two states have been reported. The fine structure of the $a^3\Sigma_u^+$ state is known very accurately from RF measurements [26–30] and allows direct comparison with the spin-spin coupling calculated in this study. To date, only one early theoretical treatment of the fine

* Dedicated to Prof. Dr. Wilfried Meyer on the occasion of his 60th birthday

Correspondence to: P. Palmieri

structure [31] and a more recent calculation of the spin-forbidden $a^3\Sigma_u^+ - X^1\Sigma_g^+$ transition [23] have been reported. The splittings and the fine structure constants of the $b^3\Pi_g$ state are also known from experiments [17, 19].

In Sect. 2, we describe the theoretical methods used in the present work; the fine structures of the atomic states of He and He^- is discussed in Sect. 3.1, of the $a^3\Sigma_u^+$ and $b^3\Pi_g$ states of He_2 in Sect. 3.2, and of the $^4\Pi_g$ state of the He_2^- in Sect. 3.3.

2 The theoretical approach

To evaluate theoretically the atomic and the molecular energies and the spectroscopic constants, the large basis set of contracted *spdf* (V5Z) Gaussian atomic orbitals of Dunning [32–34] has been augmented by diffuse orbitals on each atom and at the center of the diatomic molecules He_2 and He_2^-. The exponents for the atoms were chosen by calibrating the theoretical values of the atomic energies and constants against experiment: {*s*: 0.066, 0.026; *p*: 0.19, 0.076, 0.03, 0.01; *d*: 0.37, 0.15, 0.06, 0.024; *f*: 0.68, 0.27}. The exponents selected at the bond center of the molecule are {*s*: 0.01, 0.004; *p*: 0.004, 0.0016; *d*: 0.01}. The internally contracted MRCI [10, 11] calculations start from reference wavefunctions including all configurations of the active CASSCF $4\sigma_g$, $2\pi_{ux}$, $2\pi_{uy}$, $4\sigma_u$, $2\pi_{gx}$, $2\pi_{gy}$ molecular or corresponding atomic orbitals, respectively. Each electronic state has been optimized separately [35, 36] and all electrons were correlated. The MRCI approach was used to calculate the potential energy function for the He_2 electronic states, whereas the MRCI energies [37] for the potential energy function of the He_2^- ion are corrected by adding the Davidson corrections (cf. Sect. 3.3). All CASSCF-MRCI computations were performed using the MOLPRO program code [38].

Since the accurate evaluation of the spin-orbit and spin-spin interaction matrix elements required for this problem is better performed using the algorithm of [12] based on determinants, independent accurate expressions of all atomic and molecular wavefunctions were obtained using the determinants built from the subset of $11\sigma_g$, $6\pi_{ux}$, $6\pi_{uy}$, $2\delta_g$, $10\sigma_u$, $5\pi_{gx}$, $5\pi_{gy}$, $2\delta_u$ natural orbitals obtained for each state from the MRCI calculations. All determinants with coefficients greater than 10^{-6} were retained in the final expansions, leading essentially to a full CI [39, 40] type of wavefunctions for the subset of natural orbitals selected for each state.

We used the cartesian representation for the two operators, which are written [41]

$$\mathbf{H}_{LS} = \sum_{\mu=x,y,z} \mathbf{H}_{L_\mu S_\mu}$$
$$\mathbf{H}_{L_\mu S_\mu} = \sum_i \mathbf{h}_\mu(\mathbf{r}_i)\mathbf{S}_\mu(s_i) + \sum_{i\neq j} \mathbf{g}_\mu(\mathbf{r}_i,\mathbf{r}_j)\mathbf{S}_\mu(s_i) \quad (1)$$

$$\mathbf{H}_{SS} = \sum_{\mu,\nu=x,y,z} \mathbf{H}_{S_\mu S_\nu}$$
$$\mathbf{H}_{S_\mu S_\nu} = \sum_{i\neq j} \mathbf{g}_{\mu\nu}(\mathbf{r}_i,\mathbf{r}_j)\mathbf{S}_{\mu\nu}(s_i,s_j) \quad (2)$$

where $\mathbf{r}_i, s_i$ are the spatial and the spin coordinates of the ith electron and $\mathbf{x}_i$ is a collective symbol for the ensemble of the two sets of coordinates, i.e. $\mathbf{x}_i \equiv \{\mathbf{r}_i, s_i\}$. We follow the notation of [42–44], where $\mathbf{h}_\mu$, $\mathbf{g}_\mu$, $\mathbf{g}_{\mu\nu}$ are one- and two-electron operators in the orbital and $\mathbf{S}_\mu$, $\mathbf{S}_{\mu\nu}$ in the spin variables.

Given the electron indistinguibility, the one- and two-electron energy terms contributing to the matrix elements (1), (2), are written [12, 45]

$$h^\mu_{M,M'} = \int \mathbf{S}_\mu(s_1)\,\mathrm{d}s_1 \int \mathbf{h}_\mu(\mathbf{r}_1)\gamma_{M,M'}(\mathbf{x}'_1,\mathbf{x}_1)\,\mathrm{d}\mathbf{r}_1$$
$$g^\mu_{M,M'} = \int \mathbf{S}_\mu(s_1)\,\mathrm{d}s_1\,\mathrm{d}s_2 \int \mathbf{g}_\mu(\mathbf{r}_1,\mathbf{r}_2)\Gamma_{M,M'} \times (\mathbf{x}'_1,\mathbf{x}_1;\mathbf{x}'_2,\mathbf{x}_2)\,\mathrm{d}\mathbf{r}_1\,\mathrm{d}\mathbf{r}_2$$
$$g^{\mu\nu}_{M,M'} = \int \mathbf{S}_{\mu\nu}(s_1,s_2)\,\mathrm{d}s_1\,\mathrm{d}s_2 \int \mathbf{g}_{\mu\nu}(\mathbf{r}_1,\mathbf{r}_2)\Gamma_{M,M'} \times (\mathbf{x}'_1,\mathbf{x}_1;\mathbf{x}'_2,\mathbf{x}_2)\,\mathrm{d}\mathbf{r}_1\,\mathrm{d}\mathbf{r}_2 \quad (3)$$

All separate spin components of the electron density functions $\gamma_{M,M'}(\mathbf{x}'_1,\mathbf{x}_1)$ and $\Gamma_{M,M'}(\mathbf{x}'_1,\mathbf{x}_1;\mathbf{x}'_2,\mathbf{x}_2)$ [45] are required for the evaluation of the matrix elements (3). However, symmetry relations reduce considerably the number of the required components and simplify the evaluation of the matrix elements [12] for our full CI type of wavefunctions built on determinants.

By equating the values of each matrix element to the expression of the matrix element of the corresponding phenomenological Hamiltonian for the spin-orbit or spin-spin interactions [46, 47]

$$\mathbf{H}_{LS} = A\mathbf{L}\cdot\mathbf{S}\ , \quad (4)$$

$$\mathbf{H}_{SS} = \epsilon(3\mathbf{S}_z^2 - \mathbf{S}^2)\delta_{\Lambda,\Lambda'} + \beta(\mathbf{S}_y\mathbf{S}_z + \mathbf{S}_z\mathbf{S}_y)\delta_{\Lambda,\Lambda'\pm1} + \alpha(\mathbf{S}_x\mathbf{S}_y + \mathbf{S}_y\mathbf{S}_x)\delta_{\Lambda,\Lambda'\pm2} \quad (5)$$

one obtains the values needed for the comparison with the experimental constants and the fine structure splittings.

By using the notation for the real components of the atomic and molecular multiplets

$$^3\mathrm{P}_{x(y,z),M_S},\ ^4\mathrm{P}_{x(y,z),M_S},\ ^3\Pi_{x(y),\Sigma},\ ^4\Pi_{x(y),\Sigma} \quad (6)$$

and

$$\epsilon_S, \epsilon_P, A_P, \epsilon_P^-, A_P^-, \epsilon_\Sigma, \epsilon_\Pi, \alpha_\Pi, A_\Pi, \epsilon_\Pi^-, \alpha_\Pi^-, A_\Pi^- \quad (7)$$

for spectroscopic parameters, the following expressions are obtained for the spin-orbit and the spin-spin constants:

$a^3\Sigma^+$:

$$\epsilon_\Sigma = \tfrac{3}{2}\langle a^3\Sigma^+_{u,0,1}|\mathbf{H}_{S_zS_z}|a^3\Sigma^+_{u,0,1}\rangle$$

$b^3\Pi_g$:

$$A_\Pi = -\mathrm{i}\langle b^3\Pi_{g,x,1}|\mathbf{H}_{L_zS_z}|b^3\Pi_{g,y,1}\rangle \quad (8)$$
$$\epsilon_\Pi = \tfrac{3}{2}\langle b^3\Pi_{g,x,1}|\mathbf{H}_{S_zS_z}|b^3\Pi_{g,x,1}\rangle$$
$$\alpha_\Pi = 12\langle b^3\Pi_{g,x,1}|\mathbf{H}_{S_xS_x}|b^3\Pi_{g,x,1}\rangle - 3\langle b^3\Pi_{g,x,1}|\mathbf{H}_{S_zS_z}|b^3\Pi_{g,x,1}\rangle$$

$^4\Pi_g$:

$$A_\Pi^- = -i\tfrac{2}{3}\langle 4\Pi_{g,x,\frac{3}{2}}|\mathbf{H}_{L_zS_z}|^4\Pi_{g,y,\frac{3}{2}}\rangle$$
$$\epsilon_\Pi^- = \tfrac{1}{2}\langle^4\Pi_{g,x,\frac{3}{2}}|\mathbf{H}_{S_zS_z}|^4\Pi_{g,x,\frac{3}{2}}\rangle$$
$$\alpha_\Pi^- = 4\langle^4\Pi_{g,x,\frac{3}{2}}|\mathbf{H}_{S_xS_x}|^4\Pi_{g,x,\frac{3}{2}}\rangle - \langle^4\Pi_{g,x,\frac{3}{2}}|\mathbf{H}_{S_zS_z}|^4\Pi_{g,x,\frac{3}{2}}\rangle$$

At dissociation:

$$\begin{aligned}
&He_2(^3\Sigma_u^+) \rightarrow He(^1S) + He(^3S)\\
&He_2(^3\Pi_g) \rightarrow He(^1S) + He(^3P_g)\\
&He_2^-(^4\Pi_g) \rightarrow He(^1S) + He^-(^4P_g)
\end{aligned} \tag{9}$$

The phenomenological Hamiltonians reduce to sums of the atomic contributions, which, using the spin-orbit and the spin-spin constants A_Π, A_Π^-, ϵ_P, ϵ_P^- of the diatomic and atomic fragments (Eq. 9) are written

$$\begin{aligned}
&A_\Pi \mathbf{L}\cdot\mathbf{S} = A_P \mathbf{L}\cdot\mathbf{S}\\
&A_\Pi^- \mathbf{L}\cdot\mathbf{S} = A_P^- \mathbf{L}\cdot\mathbf{S}\\
&\epsilon_\Pi(3\mathbf{S}_z^2 - \mathbf{S}^2) = (\epsilon_S + \epsilon_P)(3\mathbf{S}_z^2 - \mathbf{S}^2)\\
&\epsilon_\Pi^-(3\mathbf{S}_z^2 - \mathbf{S}^2) = (\epsilon_S + \epsilon_P^-)(3\mathbf{S}_z^2 - \mathbf{S}^2)
\end{aligned} \tag{10}$$

By writing the asymptotic expressions of the molecular wavefunctions as products of the appropriate atomic factors

$$\begin{aligned}
&^3\Pi_{\Lambda,\Sigma} = {}^3P^1_{\Lambda,\Sigma}S_{0,0}\\
&^4\Pi_{\Lambda,\Sigma} = {}^4P^1_{\Lambda,\Sigma}S_{0,0}
\end{aligned} \tag{11}$$

we obtain the asymptotic values of the spin-orbit

$$\begin{aligned}
&A_\Pi = A_P\\
&A_\Pi^- = A_P^-
\end{aligned} \tag{12}$$

and spin-spin constants

$$\begin{aligned}
&\epsilon_\Pi = \epsilon_P\\
&\epsilon_\Pi^- = \epsilon_P^-\\
&\alpha_\Pi = 6\epsilon_P\\
&\alpha_\Pi^- = 6\epsilon_P^-
\end{aligned} \tag{13}$$

and the relationships between the atomic and the molecular constants, which have been useful to verify all definitions and the correct asymptotic behavior of our matrix elements.

3 Results and Discussion

3.1 Dissociation limits

The $a^3\Sigma_u^+$ and $b^3\Pi_g$ states of He_2 dissociate adiabatically into a ground and an excited He atom in the 2^3S or 2^3P state, respectively. Table 1 compares the computed and the experimental energies of these two triplet atomic states [48]. The calculated energies, relative to the ground state of He, are only 97 and 95 cm^{-1} lower than experiment and the calculated energy difference between the two states agrees with experiment within 2 cm^{-1}.

The fine-structure splitting of the He 2^3P state is also very well reproduced, the deviations from the experimental splittings being 0.006 cm^{-1} or 180 MHz. The calculated spin-orbit and spin-spin parameters, A and ϵ, deviate from experiment by 2% and 0.2%, respectively.

The $^4\Pi_g$ state of He_2^- dissociates adiabatically into the ground state He atom and a He^- ion in the ^4P state. The results of the present calculations for the atomic state of the negative ion He^- are summarized in Table 2. The energy of the metastable He^- $^4P_{\frac{5}{2}}$ state has been recently measured [6] to be 77.519 meV or 625.21 cm^{-1} below the 2^3S state of the neutral He atom. Our value of 615 cm^{-1} is slightly less accurate than the best atomic ab initio value of 625.22 cm^{-1}, which has been obtained by a theoretical approach specially designed for atoms [6].

The calculated fine-structure splittings in He^- agree very well with the splittings measured by Mader and Novick [2]. As for the neutral He atom, the calculation is very accurate for the spin-spin parameter, ϵ, and slightly less accurate for the spin-orbit parameter, A, presumably because of the remaining deficiencies of our contracted basis set in close proximity to the two nuclei, a small region of space which gives larger contributions to the

Table 1. Computed (a) and experimental (c) energies of the ^3S and ^3P excited states of He, relative to the ground ^1S state. Spin-orbit A_P and spin-spin ϵ_P constants and fine-structure $^3P_2$, $^3P_1$, $^3P_0$ energies in cm^{-1}. Comparison of the fine-structure constants and energies computed for the excited multiplets (a) ^3P of He and (b) $^3\Pi_g$ of He_2 at $R = 12\ a_0$, close to the asymptotic dissociation limit, with (c) the experimental values. Spin-orbit A_P and spin-spin constants ϵ_P defined by Eqs. (12), (13), (8). Experimental values from [48]

	(a)	(b)	(c)
^3S	159759		159856
^3P	168992		169087
A_P	−0.2002	−0.2044	−0.1965
ϵ_P	0.0529	0.0532	0.0528
$^3P_2 = A_P + \epsilon_P$	−0.1473	−0.1512	−0.1437
$^3P_1 = -A_P - 5\epsilon_P$	−0.0643	−0.0616	−0.0673
$^3P_0 = -2A_P + 10\epsilon_P$	0.9294	0.9408	0.9206

Table 2. Computed (a) and experimental (c) energies and electron affinity (EA) of the ^4P multiplet of He^-, relative to the ground ^1S and lowest excited ^3S state of He, respectively. Spin-orbit A_P^- and spin-spin ϵ_P^- constants and fine structure $^4P_{\frac{5}{2}}$, $^4P_{\frac{3}{2}}$, $^4P_{\frac{1}{2}}$ energies in cm^{-1}. Comparison of the fine structure constants and energies computed for the excited (a) ^4P atomic multiplet of He^- and for (b) the $^4\Pi_g$ molecular multiplet of He_2^- at $R = 10.0\ a_0$, close to the dissociation asymptotic limit with (c) the experimental values from [6]. Spin-orbit A_P^- and spin-spin constants ϵ_P^- defined by Eqs. (12), (13), (8)

	(a)	(b)	(c)
^4P	159144		159231
EA	615		625.228 ± 0.001
A_P^-	−0.0526	−0.0517	−0.0518
ϵ_P^-	0.0068	0.0065	0.0068
$^4P_{\frac{5}{2}} = \frac{3}{2}A_P^- + 3\epsilon_P^-$	−0.0584	−0.0580	−0.0573
$^4P_{\frac{3}{2}} = -A_P^- - 12\epsilon_P^-$	−0.0295	−0.0267	−0.0298
$^4P_{\frac{1}{2}} = -\frac{5}{2}A_P^- + 15\epsilon_P^-$	0.2341	0.2275	0.2316

spin-orbit, compared to spin-spin, matrix elements, and constants.

3.2 *The neutral* He_2 *molecule*

The results of the present calculations for the $a^3\Sigma_u^+$ and the $b^3\Pi_g$ states of neutral He_2 are listed in Table 3. In both cases the Davidson corrections of the variational MRCI energies were found to give negligible contributions to the potential energies and functions, indicating that our MRCI energies for He_2 are to a good precision size consistent. The $a^3\Sigma_u^+$ state potential has a barrier with a maximum of 505 cm^{-1} at $R = 5.13\ a_0$, improving, compared to previous theoretical values [21–24, 49, 50], the agreement with the experimental barrier of 500 cm^{-1} determined from scattering measuraments of $He(2^3S)$ on $He(1^1S)$ [49]. The $b^3\Pi_g$ state has no such barrier. The separation between the $a^3\Sigma_u^+$ state and the $b^3\Pi_g$ state at $R = 12\ a_0$ is 9232.5 cm^{-1}, which agrees very well with the experimental splitting between the 2^3S and 2^3P states of the He atom: 9230.9 cm^{-1}. By extrapolation of the two potentials to infinite nuclear separation, we estimate the theoretical splitting to be 9234.42 cm^{-1}.

The spin-orbit and spin-spin constants of the two states are displayed as functions of the internuclear distance in Fig. 1. Our values show that the spin-orbit function for the $b^3\Pi_g$ state, particularly, cannot be approximated by a linear function of R in the molecular region of the low-lying vibrational levels.

By solving the radial Schroedinger equation with the potentials listed in Table 3, we obtain the rovibrational energies of the $a^3\Sigma_u^+$ and $b^3\Pi_g$ states and the rovibrational averages of the spin-spin and spin-orbit coupling parameters for the fine structure of the spectroscopic levels.

The He_2 molecule has been extensively studied by spectroscopy over a wide range of frequencies. Of interest for the comparison with our results are those of

Table 3. Multireference configuration interaction (MRCI) potential energies E_Σ, E_Π and full configuration interaction spin-orbit A_Π and spin-spin $\epsilon_\Sigma, \epsilon_\Pi, \alpha_\Pi$ coupling functions for the $a^3\Sigma_u^+$ and $b^3\Pi_g$ states of He_2 with the definitions given by Eq. (8). Energies E_Σ, E_Π and R in atomic units, $\epsilon_\Sigma, \epsilon_\Pi, A_\Pi, \alpha_\Pi$ in cm^{-1}

	$a^3\Sigma_u^+$			$b^3\Pi_g$		
R	E_Σ	ϵ_Σ	E_Π	A_Π	ϵ_Π	α_Π
1.1	−4.878875	−0.057343	−4.839147	−0.209512	0.034475	0.331159
1.2	−4.963409	−0.053700	−4.927436	−0.229149	0.036597	0.330103
1.3	−5.025361	−0.049835	−4.992411	−0.240697	0.037826	0.327185
1.4	−5.070143	−0.045889	−5.039688	−0.246984	0.038448	0.323119
1.5	−5.101802	−0.041985	−5.073439	−0.249708	0.038645	0.318340
1.6	−5.123431	−0.038177	−5.096841	−0.250111	0.038571	0.313258
1.7	−5.137424	−0.034513	−5.112342	−0.248988	0.038334	0.308091
1.8	−5.145645	−0.031023	−5.121845	−0.246794	0.038012	0.302977
1.9	−5.149547	−0.027722	−5.126829	−0.244041	0.037741	0.298051
2.0	−5.150264	−0.024620	−5.128449	−0.240920	0.037394	0.293428
2.1	−5.148680	−0.021718	−5.127605	−0.237445	0.037088	0.289174
2.2	−5.145485	−0.019012	−5.124995	−0.233654	0.036842	0.285344
2.3	−5.141210	−0.016495	−5.121160	−0.229711	0.036626	0.282064
2.4	−5.136264	−0.014165	−5.116517	−0.226161	0.036546	0.279193
2.5	−5.130963	−0.012020	−5.111384	−0.222773	0.036552	0.276816
2.6	−5.125542	−0.010047	−5.106003	−0.219591	0.036647	0.274936
2.8	−5.115005	−0.006641	−5.095173	−0.214011	0.037102	0.272676
3.0	−5.105554	−0.003894	−5.084967	−0.209503	0.037875	0.272234
3.2	−5.097596	−0.001782	−5.075847	−0.206081	0.038908	0.273382
3.4	−5.091224	−0.000223	−5.067989	−0.203728	0.040147	0.275914
3.6	−5.086338	0.000783	−5.061400	−0.202291	0.041489	0.279461
3.8	−5.082734	0.001480	−5.055994	−0.201521	0.042891	0.283573
4.0	−5.080170	0.001902	−5.051635	−0.201276	0.044268	0.287935
4.2	−5.078411	0.002143	−5.048171	−0.201379	0.045564	0.292251
4.4	−5.077257	0.002334	−5.045449	−0.201686	0.046739	0.296311
4.6	−5.076544	0.002434	−5.043329	−0.202088	0.047777	0.299983
4.8	−5.076146	0.002473	−5.041690	−0.202479	0.048667	0.303154
5.0	−5.075970	0.002449	−5.040428	−0.202867	0.049430	0.305906
5.6	−5.076161	0.002118	−5.038149	−0.203870	0.051064	0.311860
6.0	−5.076528	0.001755	−5.037379	−0.204285	0.051745	0.314333
6.4	−5.076913	0.001408	−5.036924	−0.204510	0.052200	0.315949
6.8	−5.077255	0.001071	−5.036651	−0.204642	0.052510	0.317037
7.2	−5.077534	0.000790	−5.036484	−0.204685	0.052717	0.317747
7.6	−5.077748	0.000550	−5.036381	−0.204680	0.052858	0.318219
8.0	−5.077907	0.000392	−5.036315	−0.204647	0.052954	0.318531
8.4	−5.078020	0.000274	−5.036272	−0.204618	0.053020	0.318749
8.8	−5.078100	0.000189	−5.036244	−0.204587	0.053067	0.318898
9.2	−5.078154	0.000123	−5.036224	−0.204558	0.053099	0.319001
10.0	−5.078213	0.000064	−5.036201	−0.204507	0.053142	0.319134
12.0	−5.078246	0.000012	−5.036180	−0.204391	0.053161	0.319122

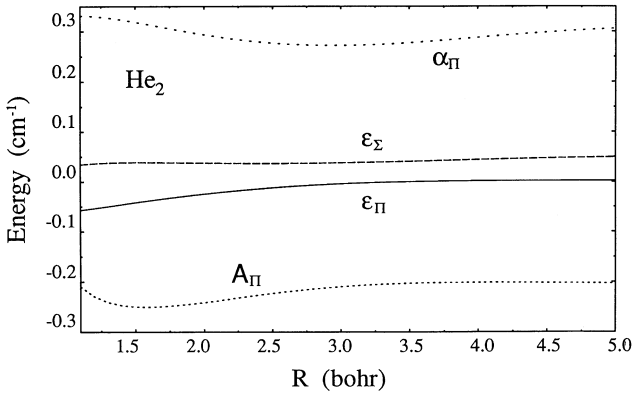

Fig. 1. ϵ_Σ, A_Π, ϵ_Π, and α_Π spin-spin and spin-orbit functions for the $a^3\Sigma_u^+$ and $b^3\Pi_g$ states of He_2

Ginter and collaborators [17, 18], which cover the UV, visible and the near-IR spectral regions with a resolution that allows accurate measurements of the vibrational and rotational structure, but with little information on the electronic fine-structure; the IR emission spectra recorded by Rogers et al. [19], which reveal the fine structure of the electronic $a^3\Sigma_u^+ \leftarrow b^3\Pi_g$ transitions; and RF measurements [26–30], which provide extremely accurate values of the electronic fine-structure splittings in the $a^3\Sigma_u^+$ state.

When comparing the results of theoretical calculations with experiment, it is important to consider the definition of the "molecular constants" and the model adopted for the analysis of the spectroscopic data. For instance, Ginter [17] analyzed the spectroscopic data of the $b^3\Pi_g$ state using two different rotational constants, one for each of the two Λ-doubling components. In the adiabatic approximation, commonly used for the solutions of the electronic problem, the potentials and the equilibrium geometries for the two states are obviously identical and, therefore, the constants obtained in [17] should be regarded simply as convenient parameters for the representation of the spectroscopic data. Only the rotational constant obtained for the Π^- component can be related to our values, since the constant for the Π^+ component is considerably modified by the coupling with the nearby $c^3\Sigma_g^+$ state induced by rotation.

These couplings have been discussed in detail by Zare et al. [47], who describes a procedure to analyze the molecular spectra in terms of "mechanical" parameters related to the potential and "electronic" parameters related to spin couplings and to non-adiabatic perturbations from other electronic states. The latter are described in the "unique perturber approximation", which assumes that only one effective electronic state contributes to the perturbation parameters. This assumption is probably adequate for the $b^3\Pi_g$ state, for which the dominant perturber is most likely the nearby $c^3\Sigma_g^+$ state. This is confirmed by a simple estimate of the Λ-doubling: assuming that both the $b^3\Pi_g$ state and the $c^3\Sigma_g^+$ state have electronic p-character and thus $L = 1$, the Λ-doubling parameter q can be estimated using the rotational constant, B, and the separation between the two states. This estimate gives $q = -0.031$ cm^{-1}, in good agreement with the experimental value of $q = -0.0254$ cm^{-1} [19].

Brown et al. [51] suggested an alternative set of parameters, avoiding implicit assumptions in the representation of the experimental spectra. The advantage is a more direct representation of the spectroscopic data; however, the experimental parameters obtained have no well-defined relationship with the "mechanical" and "electronic" parameters obtained from calculations using the Born-Oppenheimer separation of electronic and nuclear motions. Actually, only fully non-adiabatic calculations can be compared directly with spectroscopic data. The "unique perturber approximation" attempts to eliminate the non-adiabatic couplings, thus bridging the gap between potentially accurate (non-adiabatic) experiments and inherently approximate (adiabatic) theoretical calculations.

Within the "unique perturber approximation", the parameters defined by [51] have simple linear relationships with the "mechanical" and "electronic" parameters of [47]. The difference between the two ways of analyzing the spectra is quite significant. For instance, the analysis in [19] gives $B = 7.323494$ cm^{-1}, which by applying the "unique perturber approximation" is changed into $B = 7.33619$ cm^{-1}. The latter value agrees well with the value of $B = 7.337$ found by Ginter [17] for the Π^- component of the $b^3\Pi_g$ state, which should be little affected by rotational couplings to other states.

Table 4 gives a comparison of the calculated and experimental "mechanical" parameters. Both the vibrational separations and the rotational constants agree with experiment, with relative deviations of 10^{-3}. The computed wavenumbers of transitions between the $a^3\Sigma_u^+$ and $b^3\Pi_g$ states are approximately 9.5 cm^{-1} higher than experiment. This difference is to a large extent independent of the vibrational quantum number, so that a simple shift of the computed energies is sufficient for the accurate reproduction of all transition energies and representation of the spectrum.

The fine-structure transitions of the rovibrational levels of the $a^3\Sigma_u^+$ state have been measured to a precision of a few kHz using RF techniques. Table 5 collects

Table 4. Computed and experimental "mechanical" parameters of the $a^3\Sigma_u^+$ and the $b^3\Pi_g$ states of He_2: (a) [18], (b) [17], (c) [20]; the b-state rotational constant is obtained by applying the "unique perturber approximation"; see Sect. 3.2

	$a^3\Sigma_u^+$			$b^3\Pi_g$		
	Theory	(a)	(c)	Theory	(b)	(c)
B_0	7.5833	7.5890	7.58914	7.3301	7.337	7.33613
B_1	7.3429	7.3490	7.34874	7.1070	7.114	7.11298
B_2	7.0955	7.101		6.8806	6.888	
B_3	6.8398	6.846		6.6506	6.657	
B_4	6.5742	6.583		6.4166		
B_5	6.2965	6.304		6.1782		
$\Delta G_{1/2}$	1730.35	1732.14		1697.04	1698.87	
$\Delta G_{3/2}$	1652.46	1654.31		1626.59	1628.39	
$\Delta G_{5/2}$	1572.74	1574.67		1555.73	1557.62	
$\Delta G_{7/2}$	1490.79	1492.76		1484.38		
$\Delta G_{9/2}$	1406.08	1408.1		1412.44		

Table 5. Radiofrequency transitions ν_1, ν_2 (MHz), experimental spin-spin ϵ and spin-rotation γ constants in the $a^3\Sigma_u^+$ state. Difference $\Delta\epsilon$ between the observed and the computed values of the spin-spin coupling constant ϵ

v	N	ν_1	ν_2	ϵ	γ	$\Delta\epsilon$	Ref.
0	1	873.668	2199.968	−732.516	−2.421	6.361	[26]
0	3	964.992	1323.911	−731.202	−2.413	6.350	[26]
0	5	994.533	1227.021	−728.832	−2.403	6.340	[28]
0	7	1004.886	1188.718	−725.416	−2.385	6.320	[29]
0	9	1006.217	1166.449	−720.960	−2.360	6.289	[29]
0	11	1002.167	1150.073	−715.412	−2.333	6.305	[29]
0	25	901.965	1042.360	−648.276	−2.002	5.920	[30]
0	27	880.956	1022.314	−634.649	−1.939	5.852	[30]
0	29	858.607	1000.634	−620.013	−1.871	5.786	[30]
1	25	841.777	973.401	−605.220	−1.880	5.769	Present work
1	27	820.326	952.743	−591.237	−1.819	5.686	Present work
2	7	889.333	1052.009	−641.995	−2.111	6.033	[30]
2	9	889.493	1031.205	−637.352	−2.091	6.001	[30]
2	11	884.666	1015.347	−631.615	−2.065	5.968	[30]
2	19	836.513	957.42	−597.826	−1.915	5.783	Present work
3	9	829.32					Present work
3	11	824.01	945.99	−588.399	−1.934	5.776	Present work

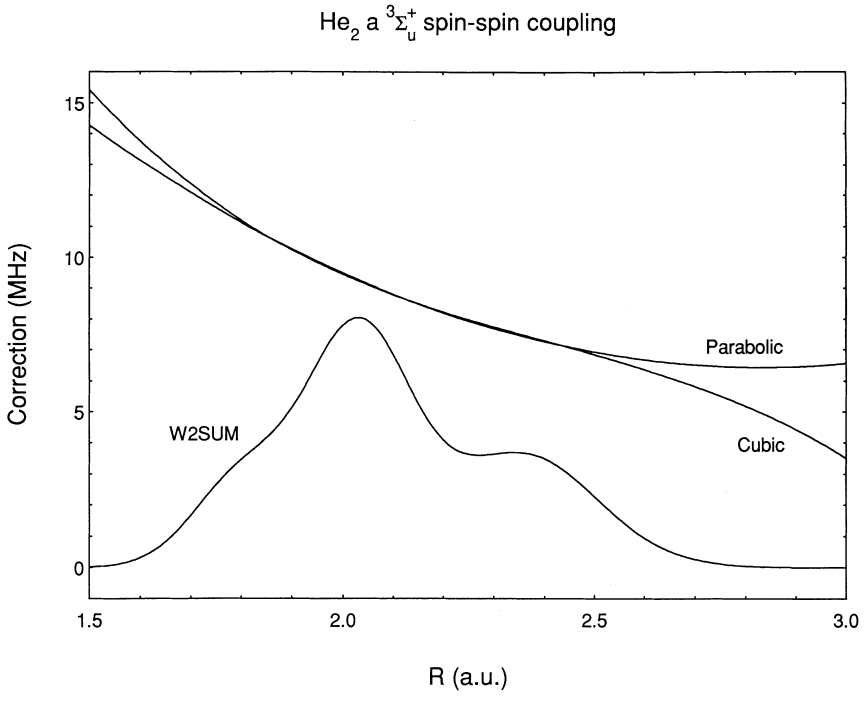

Fig. 2. Comparison of the theoretical and experimental spin-spin functions for the $a^3\Sigma_u^+$ state of He_2; parabolic and cubic empirical corrections $\Delta\lambda(R)$ to the theoretical spin-spin function $\lambda(R) = \frac{3}{2}\epsilon(R)$, Eq. (14). Sum of the squared vibrational wavefunctions, W2SUM, divided by four, to be represented on the MHz scale used for the corrections and shows the internuclear distances probed by the experiments. The parabolic and the cubic correction functions are very close in the range where W2SUM is appreciably different from zero

the RF measurements and the corresponding values of the spin-spin coupling parameter ϵ, which are compared with the rovibrational averages of the spin-spin coupling function $\epsilon(R)$ in Table 3.

The good agreement with experiment, better than 1% throughout, suggests an alternative analysis of the experimental frequencies. We start from the computed spin-spin coupling function $\epsilon(R)$ in Table 3 and introduce an empirical polynomial function $\Delta\epsilon(R)$ to correct the ab initio values and fit the experimental values of ϵ. As shown by the comparison in Fig. 2, the simple cubic polynomial correction, in MHz

$$\Delta\epsilon(R) = \tfrac{2}{3}\left[8.80584 - 6.07472x + 5.10551x^2 - 5.19396x^3\right] \tag{14}$$

where $x = (R/a_0 - 2.1)$, represents all experimental values of ϵ with a root mean square deviation of only 11 kHz, which is very close to the experimental uncertainty. This representation is advantageous from a theoretical as well as from an experimental point of view. Theoretically, the correcting polynomial represents the deviation between theory and experiment for the R-values that are probed in the experiment. Experimentally, the advantage is a very compact representation of the experimental data, requiring only four adjustable parameters to reproduce the spin-spin coupling for a large number of rotational and vibrational states. The usual representation in terms of ϵ_v constants and additional centrifugal parameters would require a much larger set of parameters. These might reproduce the available

spectra accurately but would be of little value to predict the fine structure in neighboring vibrational levels.

The fine structure in the two lowest vibrational levels of the $b^3\Pi_g$ state has been studied by IR spectroscopy [19]. Here we shall use an improved analysis based on recent extensions of the available spectroscopic data, which P. F. Bernath has kindly communicated to us [20]. The experimental and theoretical fine-structure parameters are compared in Table 6. As found for the atomic fine-structure parameters, the spin-spin coupling is computed more accurately compared with the spin-orbit coupling: our spin-orbit constant, A, is 6% larger than the experimental value, whereas the two spin-spin coupling constants, ϵ and α, are extremely close to the experimental values.

3.3 The He_2^- *molecular ion*

The potentials and the fine-structure parameters computed for the $^4\Pi_g$ state of He_2^- are listed in Table 7. Compared to the neutral molecule, the Davidson corrections for the MRCI energies are more important and approximately two orders of magnitude larger; they have been added to the MRCI energies to restore, approximately, their size consistency. The importance of this correction is demonstrated by the asymptotic value of the electron affinity, which, at $R = 10a_0$, after adding the Davidson corrections to the two energies, is shifted from the MRCI value of 448 cm^{-1} to 609 cm^{-1}, in much better agreement with the electron affinity of the He atom in the 2^3S state at dissociation, 625.22 cm^{-1}. The larger values of these corrections reflect, on one hand, the increased difficulty for the accurate theoretical description and, on the other hand, the importance of multiple excitations for the electron correlation in the negative ion compared to the neutral species. We infer that our fine-structure parameters, the spin-orbit and spin-spin coupling constants, are presumably less accurate for the negative ion than for the neutral molecule.

As shown in Fig. 3 and found in the neutral Rydberg state, the spin-orbit constant is not a linear function of R in the region of the low-lying vibrational levels.

To generate the potential for the negative ion and solve numerically the radial Schroedinger equation for the nuclear motion, we have adopted the following interpolation procedure. First, we evaluate the difference between the He_2^- $^4\Pi_g$ state and the He_2 $a^3\Sigma_u^+$ state energies, producing a smooth energy function of the internuclear distance, R, with a well-known limiting behavior for large values of R, since it converges to the electron affinity of the He atom in the 2^3S state. This function is next interpolated, and the interpolating function subsequently added to the $a^3\Sigma_u^+$ state potential, which is available on a finer grid. By this procedure, besides limiting the number of energies calculated for the negative ion (Table 7), which require much larger computational resources, we reduce the errors in the interpolation, which may become inaccurate when the potential energies are not very smooth or when they are not known at closely spaced geometries. We notice that the asymptotic barrier in the $a^3\Sigma_u^+$ potential of He_2 survives in the $^4\Pi_g$ potential of He_2^-.

We conclude from our potential that two vibrational levels of the negative ion, $v = 0$ and $v = 1$, are bound; presumably, all remaining vibrational levels of the $^4\Pi_g$ state autodetach, since they have higher energies than the $a^3\Sigma_u^+$ $(v = 0)$, state of the neutral molecule He_2.

Table 6. (a) Computed and (b) experimental fine-structure constants of the $v = 0$ and $v = 1$ $b^3\Pi_g$ states of He_2. The experimental constants are obtained from the improved analysis by P.F. Bernath of [17], using the "unique perturber approximation"

	$v = 0$		$v = 1$	
	(a)	(b)	(a)	(b)
A	−0.23934	−0.22734	−0.23689	−0.22368
ϵ	0.03730	0.03703	0.03721	0.03574
α	0.29084	0.28976	0.29043	0.28835

Table 7. E_Π^- MRCI energies including the Davidson correction, spin-orbit A_Π^-, and spin-spin $\epsilon_\Pi^-, \alpha_\Pi^-$ coupling functions for the $^4\Pi_g$ states of He_2^- with the definitions given by Eq. (8). Energies E_Π^- and R in au, $A_\Pi^-, \epsilon_\Pi^-, \alpha_\Pi^-$ in cm^{-1}

R	E_Π^-	A_Π^-	ϵ_Π^-	α_Π^-
1.2	−4.968136	−0.070730	−0.005365	0.049602
1.3	−5.030961	−0.073276	−0.004045	0.050149
1.4	−5.076495	−0.074824	−0.002883	0.050366
1.5	−5.108832	−0.075488	−0.001883	0.050254
1.6	−5.131038	−0.075788	−0.000951	0.050081
1.8	−5.154210	−0.075178	0.000644	0.049349
2.0	−5.159491	−0.073513	0.001903	0.048446
2.2	−5.155143	−0.071656	0.002984	0.047503
2.4	−5.146125	−0.069870	0.003923	0.046764
2.6	−5.135387	−0.067812	0.004729	0.045933
2.8	−5.124623	−0.066071	0.005423	0.045357
3.0	−5.114753	−0.064635	0.006027	0.044928
3.2	−5.106219	−0.063223	0.006542	0.044574
3.4	−5.099166	−0.061992	0.006945	0.044276
3.6	−5.093560	−0.060854	0.007255	0.043983
4.0	−5.085998	−0.058037	0.007515	0.042852
4.2	−5.083675	−0.057033	0.007573	0.042422
4.4	−5.082052	−0.056083	0.007553	0.041978
4.6	−5.080953	−0.055014	0.007497	0.041342
6.0	−5.079948	−0.051266	0.006947	0.038725
10.0	−5.080995	−0.051741	0.006540	0.039157

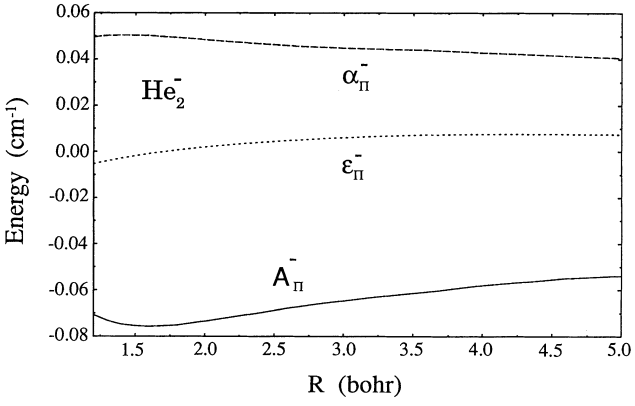

Fig. 3. A_Π^-, ϵ_Π^-, and α_Π^- spin-orbit and spin-spin functions for the $^4\Pi_g$ states of He_2^-

Table 8. Spectroscopic parameters in cm^{-1} predicted for the $v = 0$ and $v = 1$ $^4\Pi_g$ states of He_2^-

	$v = 0$	$v = 1$
B	7.49786	7.26471
D	5.492×10^{-4}	5.512×10^{-4}
H	3.2×10^{-8}	3.2×10^{-8}
A	−0.07333	−0.07275
ϵ	0.001958	0.002210
α	0.04837	0.04812

Previous theoretical studies [52–55] have reported only one bound vibrational level for He_2^-. To aid future experiments on the autoionization of the negative ion and its fine-structure levels, we report in Table 8 the spectroscopic parameters computed for the two lowest vibrational levels of He_2^-. Comparing Tables 6 and 8, we notice that both the spin-orbit and the spin-spin parameters are smaller in He_2^- than in the neutral molecule. We also note that the "off-diagonal" spin-spin parameter, α, makes a significant contribution to the fine structure in the negative ion as well as in the neutral molecule.

4 Conclusions

We have presented a detailed derivation of the fine-structure constants of the $a^3\Sigma_u^+$, $b^3\Pi_g$ states of He_2, of the $^4\Pi_g$ state of He_2^-, and of the parent atomic states using ab initio CI techniques. For the fine structure of the atomic and Rydberg molecular states a large amount of experimental information is available, allowing a detailed comparison with our values, which were found to be in very good agreement with experiment. Therefore we believe that our results represent reliable predictions for the molecular ion He_2^- and provide useful information for experimental investigations on the fine structure of the autoionizing multiplets of the ion and the identification of their long-lived component. We have proposed a modified procedure to treat the spectroscopic data of the $a^3\Sigma_u^+$ state of He_2 starting from our theoretical spin-spin coupling function, which may find useful applications for the spectroscopic data of the molecular anion He_2^-.

Acknowledgements. This work has been supported by EC grant FMRX-CT96-0088. A.O.M. acknowledges financial support from CINECA, the computer center of the University of Bologna, where most of the computations for this work have been performed. We are indebted to Professor P. F. Bernath, who kindly provided us with an improved analysis of the IR spectra of He_2 prior to publication.

References

1. Hiby W (1939) Ann Phys (NY) 34:473
2. Mader DL, Novick R (1972) Phys Rev Lett 29:199; (b) Mader DL, Novick R (1974) Phys Rev Lett 32:185
3. Andersen T, Anderssen LH, Balling P, Haugen HK, Hvelplund P, Smith WW, Taulberg K, (1993) Phys Rev A 47:890
4. Novick R, Weinflash D (1970) In: Langenberg DN, Baylor NN (eds) Proceedings of the international conference on precision and fundamental constants. (Natl Bur Stand spec publ no 343) US GPO, Washington, p 403
5. Bunge A, Bunge CF (1984) Phys Rev A 30:2179
6. Kristensen P, Pedersen UV, Petrunin VV, Andersen T, Chung KT (1997) Phys Rev A 55:978
7. Bae YK, Coggiola MJ, Peterson J (1984) Phys Rev Lett 52:747
8. Kvale TJ, Compton RN, Alton GD, Thompson JS, Pegg DJ (1986) Phys Rev Lett 56:592
9. Andersen T, Andersen LH, Bjerre N, Hvelplund P, Posthumus JH (1994) J Phys B: At Mol Opt Phys 27:1135
10. Werner H-J, Knowles PJ (1988) J Chem Phys 89:5803
11. Knowles PJ, Werner HJ (1988) Chem Phys Lett 145:514
12. Mitrushenkov AO, Palmieri P (1997) Mol Phys 92:511
13. Goldstein F (1913) Verh Dtsch Phys Ges 15:402
14. Curtis WF (1913) Proc R Soc London 89:146
15. Hepner G, Herman L (1956) C R Hebd Seances Acad Sci Paris 243:1504
16. Gloersen P, Dieke GH (1965) J Mol Spectrosc 16:191
17. Ginter ML (1965) J Mol Spectrosc 18:321
18. Brown CM, Ginter ML (1971) J Mol Spectrosc 40:302
19. Rogers SA, Brazier CR, Bernath PF, Brault JW (1988) Mol Phys 63:901
20. Bernath PF (unpublished)
21. Mulliken RS (1964) Phys Rev A 136:962
22. Guberman SL, Goddard WA (1975) Phys Rev A 12:1203
23. Yarkony D (1989) J Chem Phys 90:7164
24. (a) Konowalow DD, Lengsfield BH III (1987) Chem Phys Lett 139:417; (b) Konowalow DD, Lengsfield BH III (1987) J Chem Phys 87:4000
25. Cohen JS (1976) Phys Rev A 13:86
26. Lichten W, McCusker MV, Vierima TL (1974) J Chem Phys 61:2200
27. Vierima TL (1975) J Chem Phys 62:2925
28. Lichten W, Wik T (1978) J Chem Phys 69:98
29. Kristensen M, Bjerre N (1990) J Chem Phys 93:983
30. Hazell I, Norregaard A, Bjerre N (1995) J Mol Spectrosc 172:135
31. Beck DR, Nicolaides CA, Musher JI (1974) Phys Rev A 10:1522
32. Dunning TH Jr (1989) J Chem Phys 90:1007
33. Kendall RA, Dunning TH Jr, Harrison RJ (1992) J Chem Phys 96:6796
34. Woon DE, Dunning TH Jr (1993) J Chem Phys 98:1358
35. Werner H-J, Knowles PJ (1985) J Chem Phys 82:5053
36. Knowles PJ, Werner H-J (1985) Chem Phys Lett 115:259
37. (a) Langhoff SR, Davidson ER (1974) Int J Quantum Chem 8:61; (b) Peyerimhoff SD, Buenker RJ (1981) Chem Phys 57:279
38. Werner H-J, Knowles PJ (1997) MOLPRO, a package of ab initio programs with contributions from Almlöf J, Amos RD, Deegan MJO, Elbert ST, Hampel C, Meyer W, Peterson K, Pitzer RM, Stone AJ, Taylor PR, Lindh R, Mura ME, Thorsteinsson T, Cooper DL University of Birmingham, UK
39. Knowles PJ, Handy NC (1989) J Chem Phys 91:2396
40. Mitrushenkov AO (1994) Chem Phys Lett 217:559
41. McWeeny R (1965) J Chem Phys 42:1717
42. Bearpark MJ, Handy NC, Palmieri P, Tarroni R (1993) Mol Phys 80:479
43. Palmieri P, Tarroni R, Amos RD (1994) J Phys Chem 100:5849
44. Amos RD (1992) CADPAC, the Cambridge analytic derivatives package, issue 5. A suite of quantum chemistry programs with contributions from Alberts IL, Andrews JS, Colwell SM, Handy NC, Jayatilaka D, Knowles PJ, Kobayashi R, Koga N, Laidig KE, Maslen PE, Murray CW, Rice JE, Sanz J, Simandiras ED, Stone AJ, Su MD. University of Cambridge, UK
45. McWeeny R (1960) Rev Mod Phys 32:335
46. Kovàcs I (1969) Rotational structure in the spectra of diatomic molecules. Hilger, London
47. Zare RN, Schmeltkopf AL, Harrop WJ, Albritton DL (1973) J Mol Spectrosc 46:37

48. Martin WC (1987) Phys Rev A 36:3575
49. Jordan RM, Siddiqui HR, Siska PE (1986) J Chem Phys 84:6719
50. Sunil KK, Lin J, Siddiqui H, Siska PE, Jordan KD, Shepard R (1983) J Chem Phys 78:6190
51. Brown JM, Calbourn EA, Watson JKG, Wayne FD (1979) J Mol Spectrosc 74:294
52. Michels HH (1984) Phys Rev Lett 52:1413
53. Bae YK, Peterson JR, Michels HH, Hobbs RH (1988) Phys Rev A 37:2778
54. Pluta T, Bartlett RJ, Adamowicz L (1989) Phys Rev A 40:2253
55. Adamowicz L, Pluta T (1991) Phys Rev A 44:2860